Regular article

Network pharmacology-based exploration of the synergistic efficacy and detoxification mechanisms of *Tripterygium wilfordii* and *Epimedium brevicornum* in treating rheumatoid arthritis

Yuhang Wang[a], Boyan Shen[b], Yuanqing Li[a,*], Guodong Yao[a,*]

[a] *School of Traditional Chinese Materia Medica, Shenyang Pharmaceutical University, Shenyang 110016, China;*
[b] *School of Pharmaceutical Engineering, Shenyang Pharmaceutical University, Shenyang 110016, China*

Abstract

Rheumatoid arthritis (RA) is a chronic autoimmune disease with limited therapeutic options. The herbal compatibility of *Tripterygium wilfordii* Hook. f. (Leigongteng, LGT) and *Epimedium brevicornum* Maxim. (Yinyanghuo, YYH), widely used in Traditional Chinese Medicine, has shown promising efficacy in RA treatment, yet its synergistic mechanisms and hepatoprotective effects remain unclear. In this study, we systematically investigated the therapeutic and hepatotoxicity-attenuating mechanisms of LGT-YYH using integrated network pharmacology and molecular docking approaches. Bioactive compounds and corresponding targets from LGT and YYH were retrieved from the TCMSP database, while RA- and hepatotoxicity-related targets were collected from public databases and microarray datasets. Protein-protein interaction networks, hub protein targets identification, and functional enrichment analyses revealed that 65 LGT and 26 YYH bioactive compounds collectively interact with 527 RA-related targets, with hub targets including PTPN11, SRC, EGFR, MAPK1, and MAPK8 central to the therapeutic network. KEGG enrichment highlighted the MAPK signaling pathway as a key mechanism of anti-RA activity. Furthermore, 243 targets were associated with LGT-induced hepatotoxicity, and YYH components, particularly icariin, kaempferol, and epimedin B, exhibited binding to hepatotoxicity-related targets such as AKT1 and ESR1, suggesting a hepatoprotective role via the AKT1-ESR1-Nrf2 axis. These findings indicate that LGT-YYH exerts synergistic anti-RA effects by modulating MAPK-related signaling while YYH components may mitigate LGT-induced hepatotoxicity, exemplifying the TCM principle of enhancing therapeutic efficacy while reducing toxicity.

Keywords: *Tripterygium wilfordii*; *Epimedium brevicornum*; rheumatoid arthritis; hepatoprotection; synergistic effect; network pharmacology; molecular docking

1 Introduction

Rheumatoid arthritis (RA) is a systemic autoimmune disease characterized by chronic synovial inflammation, cartilage destruction, and bone erosion, often resulting in joint deformity and functional impairment [1]. With a global prevalence of 0.5%–1%, RA management remains challenging. Current treatments—including nonsteroidal anti-inflammatory drugs, conventional disease-modifying antirheumatic drugs, and biologics—while effective,

These authors have no conflict of interest to declare.
* Author to whom correspondence should be addressed. Address: School of Traditional Chinese Materia Medica, Shenyang Pharmaceutical University, Shenyang 110016, China; Tel.: +86-24-43520707 (Yuanqing Li), E-mail: lzrzlzrz@sina.com (Yuanqing Li); Tel.: +86-24-43520707 (Guodong Yao), E-mail: guodong_yao@126.com (Guodong Yao).

are limited by delayed onset, incomplete efficacy, high cost, and significant adverse effects such as infections, hepatotoxicity, and infertility [2]. Consequently, there is an urgent need for novel therapeutic strategies that combine high efficacy with improved safety profiles.

Traditional Chinese Medicine (TCM) provides a valuable complementary approach to RA management [3]. In particular, *Tripterygium wilfordii* Hook. f. (Leigongteng, LGT) has been widely used for RA and other autoimmune diseases due to its potentantiinflammatory and immunomodulatory properties [2,4]. Systematic reviews have confirmed the efficacy of LGT preparations in improving RA symptoms [5]. However, its clinical application is substantially limited by serious adverse effects, particularly hepatotoxicity and reproductive toxicity [6-7]. Key toxic constituents, such as triptolide and celastrol, have been shown to induce liver injury by elevating ALT/AST levels and promoting oxidative stress [5,8].

Epimedium brevicornum Maxim. (Yinyanghuo, YYH) is a traditional Chinese medicinal herb rich in flavonoids such as icariin, kaempferol, and quercetin, which exert antiRA effects through immunomodulation and cartilage protection [9-10]. Among these, kaempferol has been shown to alleviate RA symptoms in a collageninduced arthritis model via modulation of the NLRP3–CASP1/GSDMD pyroptosis axis and immune cell subsets [11]. Additionally, icariin, a major flavonoid component of YYH, has demonstrated hepatoprotective properties and has attracted increasing research attention [12].

The therapeutic potential of the LGT–YYH combination is supported by clinical evidence and patented formulations. Clinical studies of compound preparations containing both herbs have demonstrated promising outcomes. For example, Jinguan Tablet employs LGT as the monarch herb (a core component in TCM) and YYH as the adjuvant herb, achieving a total effective rate of 97.7% in the treatment of active RA, with fewer adverse effects than conventional Western therapies [13]. Patented formulations further validate the efficacy of this herbal combination. Chinese Patent CN102657736A integrates LGT and YYH with other herbs for RA treatment, adhering to the TCM principle of "eliminating pathogens and reinforcing healthy qi" within a single prescription. In this formulation, LGT functions to eliminate pathogens, while YYH reinforces healthy qi. Thus, the LGT–YYH herbal compatibility represents a promising strategy for antiRA therapy, balancing therapeutic efficacy with reduced toxicity. Nevertheless, the precise molecular mechanisms underlying their synergistic effects remain incompletely understood and warrant further investigation.

Herein, we employed a network pharmacology strategy integrated with molecular docking to systematically investigate the mechanisms of the LGT–YYH herb pair in RA treatment. Active compounds were identified, human targets predicted, and disease and toxicityrelated networks constructed. Through protein–protein interaction analysis, hub target identification, and pathway enrichment, we mapped key signaling pathways associated with both RA and hepatotoxicity. Representative compounds were subsequently docked against hub targets to verify binding affinities and support mechanistic hypotheses [14]. This integrative approach provides a scientific basis for the rational clinical use of LGT–YYH in RA therapy by elucidating both its therapeutic synergy and potential toxicity mitigation.

2 Materials and methods

2.1 Screening of active ingredients and target prediction

The active components of LGT and YYH were retrieved from the Traditional Chinese Medicine

Systems Pharmacology Database (TCMSP, https://www.tcmsp-e.com/) using "*Tripterygium wilfordii*" and "*Epimedium*" as keywords. Compounds were screened based on oral bioavailability (OB ≥ 30%) and drug-likeness (DL ≥ 0.18) [15]. After cross-checking with the *Chinese Pharmacopoeia* (2025 edition), 65 and 26 bioactive components were retained for LGT and YYH, respectively.

The 3D structures of these compounds were imported into the PharmMapper server (http://www.lilab-ecust.cn/pharmmapper/) to predict potential protein targets [16], with the species limited to *Homo sapiens* and a threshold of Norm Fit ≥ 0.5. All predicted protein IDs were standardized into official *Gene Symbols* using the UniProt database (https://www.uniprot.org/) [17]. As a result, 2370 and 2100 putative targets were obtained for LGT and YYH, respectively.

2.2 Collection of RA-related targets and intersection with LGT-YYH targets

To comprehensively identify RA-associated targets, both transcriptomic and database-mining strategies were employed. The keyword "rheumatoid arthritis" was first used to search the Gene Expression Omnibus (GEO) database (https://www.ncbi.nlm.nih.gov/gds). Two microarray datasets, GSE157047 and GSE116899 [18], were selected for analysis. Differential expression analysis was performed using the GRO2R tool with the following screening criteria: $|\log2FC| > 1$ and $P < 0.05$. This was done to ensure the selection of biologically relevant genes for further analysis.

To further expand the RA-related target collection, multiple disease databases were queried using the same keyword "rheumatoid arthritis" including GeneCards (https://www.genecards.org/), Therapeutic Target Database (TTD, https://ttd.idrblab.cn/), Online Mendelian Inheritance in Man (OMIM, https://www.omim.org/), and Comparative Toxicogenomics Database (CTD, https://ctdbase.org/) [19-22]. Targets were ranked according to their relevance or inference scores, with higher scores indicating stronger associations with RA. In GeneCards, targets with a Relevance Score ≥ 5 were retained, while in CTD, those with an Inference Score ≥ 50 were included.

The jvenn online tool (http://jvenn.toulouse.inra.fr/app/example.html) was used to identify overlaps between LGT-YYH compound targets and RA-related target [23]. The resulting intersection targets were considered potential therapeutic targets of the LGT-YYH pair for RA treatment.

2.3 Collection and intersection analysis of LGT hepatotoxicity-related targets

To explore the potential hepatotoxicity mechanisms of LGT, both literature review and database-mining approaches were conducted. The keywords "Hepatotoxicity" and "Liver injury" were used to search multiple databases, including GeneCards, TTD, OMIM, CTD, and Traditional Chinese Medicine Systems Toxicology Database (TCMSTD, https://www.bic.ac.cn/TCMSTD/) [24].

All retrieved targets were ranked by their relevance or inference scores, with higher scores reflecting stronger associations with liver injury. Targets were filtered by relevance scores (GeneCards: Relevance Score ≥ 3.6; CTD: Inference Score ≥ 300).

The LGT compound targets were intersected with the hepatotoxicity targets using jvenn. The overlapping genes were considered core targets involved in LGT-induced liver injury and used for subsequent PPI and pathway analyses.

2.4 Protein-protein interaction (PPI) network and hub protein targets identification

The overlapping targets from efficacy and

toxicity analyses were imported into the STRING database (https://string-db.org/) to construct PPI networks. The species was limited to *Homo sapiens*, and a minimum interaction score of 0.7 was applied. The resulting networks were visualized and analyzed using Cytoscape (v3.10) [25-26]. The STRING interaction data were exported and subsequently re-visualized and analyzed in Cytoscape to perform network topology analysis, ensuring consistency between the visualization and hub-targets analysis.

Topological analysis was conducted using the cytoHubba plug-in, applying four centrality algorithms—Maximal Clique Centrality (MCC), Edge Percolated Component (EPC), Maximum Neighborhood Component (MNC), and Bottleneck (BN)—to evaluate the importance of each node within the network. For each protein target, ranks were normalized to a 0-1 scale across all four parameters, and a consensus score was calculated as the sum of normalized values. Protein targets with higher consensus scores were considered to play central roles in the network.

Consensus Score = normalized (MCC) + normalized (EPC) + normalized (MNC) + normalized (BN), where each metric was scaled between 0–1 before summation.

$$X^{norm} = (X_{max} - X_{min}) / (X_i - X_{min})$$

where X represents MCC, EPC, MNC, or BN.

2.5 Functional enrichment analysis

Functional enrichment analyses were conducted to explore the biological significance of the intersected targets from the efficacy and hepatotoxicity networks. For the intersection sets—LGT-YYH therapeutic targets and LGT hepatotoxicity targets—Gene Ontology (GO) and Kyoto Encyclopedia of Genes and Genomes (KEGG) pathway enrichment analyses were performed using the Database for Annotation, Visualization and Integrated Discovery (DAVID, https://david.ncifcrf.gov/) [27]. The enrichment analyses covered Biological Process (BP), Molecular Function (MF), and Cellular Component (CC) categories. Terms with $P < 0.01$ were considered statistically significant. Results were visualized as bar plots and bubble plots using the Bioinformatics online platform (http://www.bioinformatics.com.cn/).

For YYH targets, enrichment analysis was conducted using the R package *clusterProfiler* (v4.8.1) with adjusted thresholds of $P < 0.05$ and $q < 0.05$. Results were visualized using *ggplot2* and *enrichplot*. packages. The R-based approach was chosen for the YYH dataset because it provided enhanced flexibility in multiple dataset integration, reproducibility in statistical adjustment (Benjamini-Hochberg correction), and fine control over graphical presentation compared to the DAVID-based workflow. Comparative enrichment analyses were conducted between the efficacy and toxicity networks to identify overlapping or opposing pathways.

2.6 Comparative KEGG pathway analysis between LGT hepatotoxicity and YYH networks

To investigate the potential pathway-level interactions between LGT-induced hepatotoxicity and YYH, a comparative KEGG pathway analysis was conducted. The KEGG enrichment results of LGT hepatotoxicity-related targets and YYH targets were obtained from their respective enrichment analyses—LGT hepatotoxicity KEGG results were derived from the DAVID database ($P < 0.01$), while YYH target enrichment was performed using the R package clusterProfiler (v4.8.1), with adjusted thresholds of $P < 0.05$ and $q < 0.05$.

The two enrichment result tables were imported into R (version 4.3.1) for comparative analysis using the packages including *readr*, *dplyr*, *VennDiagram*, *UpSetR*, and *ggplot2*. Pathway name columns were automatically recognized from the KEGG output files, and missing or duplicate entries were removed.

A summary table containing the overlapping, LGT-specific, and YYH-specific pathways was exported.

For visualization, a Venn diagram and an UpSet plot were generated to illustrate the degree of overlap and the unique KEGG pathways associated with each network. The Venn diagram was created using the VennDiagram package, with LGT and YYH represented in red and blue, respectively, while the UpSet plot quantified intersections using the *UpSetR* package.

This comparison enabled the identification of YYH-enriched compensatory pathways that might counteract or negatively regulate LGT-induced hepatotoxic pathways, thereby revealing a potential pathway-level detoxification mechanism underlying the LGT-YYH herbal pair.

2.7 Molecular docking validation

Representative compounds were selected based on network degree values and literature support. Protein structures were downloaded from the RCSB Protein Data Bank (https://www.rcsb.org/), prioritizing high-resolution human structures. Protein and ligand preparation was performed using the Schrödinger Maestro suite. Proteins were prepared by adding hydrogens, removing water molecules, and optimizing hydrogen bonds. Ligands were energy-minimized using the OPLS3e force field.

Molecular docking was performed using Glide in standard precision (SP) mode. Grid boxes were centered on co-crystallized ligand binding sites. Docking poses were evaluated using GlideScore (GScore), with more negative values indicating stronger binding affinity. Visualization and analysis of docking poses were conducted using PyMOL.

2.8 Integrated evaluation of synergistic and hepatoprotective mechanisms

Hub targets and significantly enriched pathways from both efficacy and toxicity networks were systematically compared to identify overlapping or functionally antagonistic pathways. Protein-functional relationships were analyzed by constructing a dual-network model that integrated both therapeutic and hepatotoxic mechanisms. This model identified key regulatory nodes where YYH components may counteract LGT-induced toxicity while preserving therapeutic efficacy.

3 Results

3.1 Identification of active compounds and predicted targets

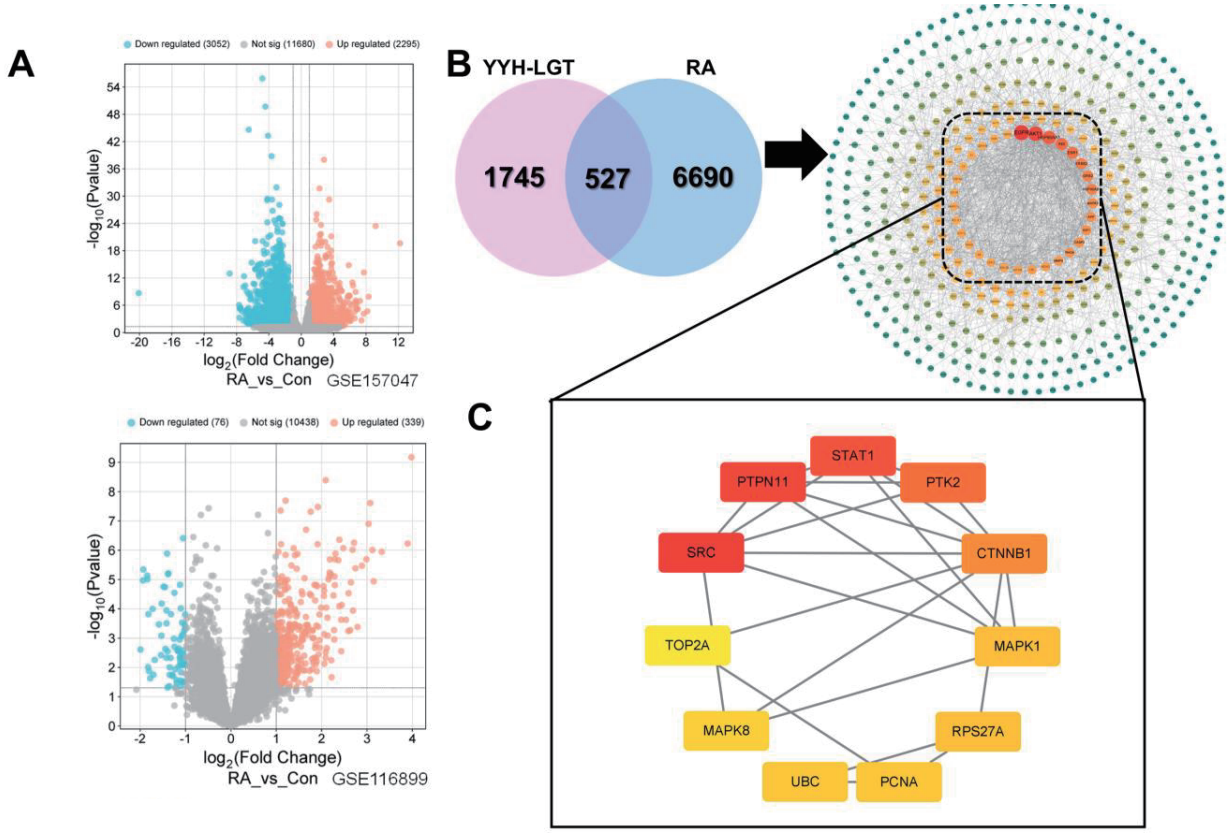
To establish the chemical basis of the LGT-YYH herbal pair, we systematically screened their bioactive components. From the TCMSP database, a total of 65 and 26 active compounds were identified from LGT and YYH, respectively, adhering to the pharmacokinetic criteria of OB ≥ 30% and DL ≥ 0.18. The ingredients of the analyzed herbs have been listed in the supporting information file. Subsequent target prediction via the PharmMapper server and unification through the UniProt database yielded 2,370 and 2,100 putative human protein targets for LGT and YYH, reflecting the broad potential interactome of these herbs. Notable representative compounds included triptolide, celastrol, kaempferol, quercetin, and icaritin, which are consistent with previously reported pharmacological profiles, supporting the relevance of our screening approach.

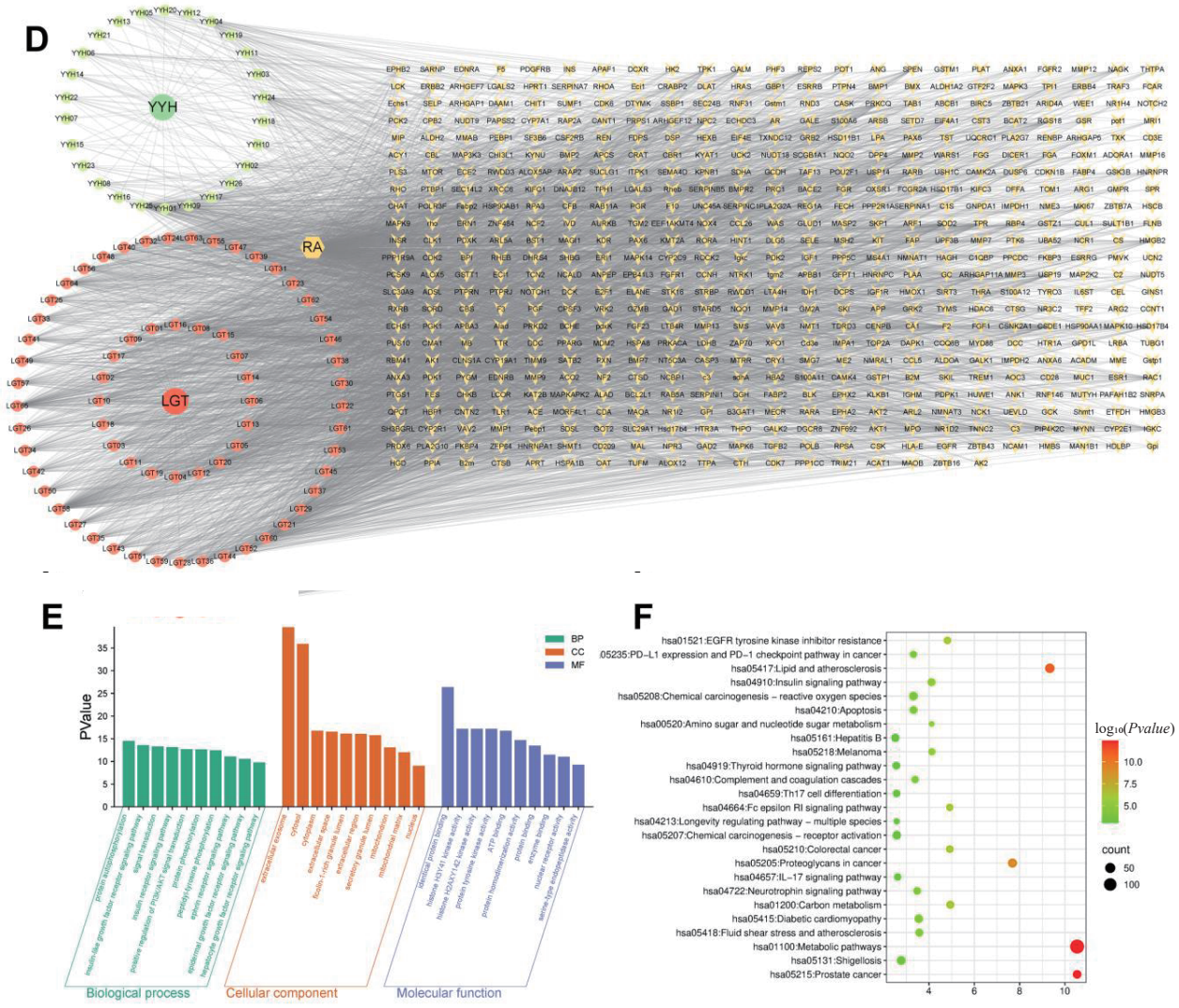
3.2 Identification of RA-related targets and intersection with LGT-YYH targets

To delineate the potential therapeutic targets of the LGT-YYH pair against RA, we first constructed a comprehensive RA-related target pool. Differential gene expression analysis of two GEO datasets

(|log2FoldChange| > 1, $P < 0.05$), GSE157047 and GSE116899, identified 5,347 and 415 significantly dysregulated genes in RA synovial tissues, respectively (Fig. 1A). Additionally, RA-related targets were retrieved using the keyword "rheumatoid arthritis" from multiple databases, including GeneCards, TTD, OMIM, and CTD. A total of 917 targets were obtained from GeneCards, 100 targets from TTD, 48 targets from OMIM, and 519 targets from CTD. After removing duplicate entries, these targets were combined with differentially expressed genes (DEGs) identified from GEO datasets to construct the RA-related gene set. In total, 7217 RA-related targets were collected. Subsequently, intersection analysis between the RA-related targets set and the predicted targets of the LGT-YYH herb pair identified 527 overlapping tavrgets, which were considered potential therapeutic targets of LGT-YYH in rheumatoid arthritis (Fig. 1B).

All the intersected targets were ranked according to their degree in the network. These targets were considered as potential therapeutic targets for the LGT-YYH herbal pair in the treatment of RA (Fig. 1B). Finally, a drug-compound-target-disease network was constructed, visually encapsulating the complex multi-component, multi-target nature of the LGT-YYH pair against RA, where compounds from both herbs converge on and modulate a shared network of disease-related proteins (Fig. 1D)





(A) Volcano plots showing differential gene expression in GSE157047 and GSE116899 datasets (RA vs. control), with upregulated genes in red, downregulated genes in blue, and non-significant genes in gray; (B) Venn diagram and PPI network of intersecting targets between LGT-YYH and RA (n = 527); nodes with higher degree values are closer to the center; (C) Top hub targets extracted based on degree values in the intersection network; (D) Drug-compound-target-disease network illustrating multi-target interactions of LGT and YYH active compounds with RA-related targets; (E) GO enrichment of top 10 terms across Biological Process, Cellular Component, and Molecular Function categories; (F) KEGG enrichment of top 20 pathways related to inflammation, immune response, apoptosis, and cell signaling; bubble size represents gene count and color intensity corresponds to $-\log_{10}(P)$.

Fig. 1 Network analysis of LGT-YYH herbal pair in RA treatment

3.3 PPI network and hub protein targets identification in RA treatment

To decipher the functional modules within the 527 overlapping targets, a protein-protein interaction (PPI) network was constructed using the STRING database (confidence score > 0.7) and visualized in Cytoscape. The resulting network exhibited significant connectivity, indicating that the targets of LGT-YYH do not act in isolation but rather as coordinated complexes.

Topological analysis using the cytoHubba plugin,

based on four centrality algorithms (MCC, EPC, MNC, and BN), identified 11 hub targets, which were identified as the core regulatory nodes of the LGT-YYH therapeutic network against RA: *PTPN11*, *SRC*, *STAT1*, *PTK2*, *PCNA*, *TOP2A*, *RPS27A*, *MAPK8*, *MAPK1*, *UBC*, and *CTNNB1*. These hub targets, including PTPN11 (SHP2), SRC, MAPK1 (ERK2), and MAPK8 (JNK1), are known master regulators of intracellular signaling. Their high centrality implies that the therapeutic effect of LGT-YYH is likely mediated through the disruption of critical inflammatory and proliferative signaling hubs (Fig. 1C).

Table 1 Hub targets identified from the PPI network of LGT-YYH therapeutic targets against rheumatoid arthritis (RA)

Rank	Protein targets symbol	Full name	Consensus score	Functional annotation	Refs
1	PTPN11	Protein Tyrosine Phosphatase Non-Receptor Type 11 (SHP2)	3.774	Tyrosine phosphatase involved in MAPK signaling, mediates cytokine and growth factor pathways.	[28]
2	SRC	SRC Proto-Oncogene, Non-Receptor Tyrosine Kinase	3.760	Regulates inflammatory signaling, cell adhesion, and proliferation; participates in TNF and FcεRI signaling.	[29]
3	STAT1	Signal Transducer and Activator of Transcription 1	3.753	Mediates interferon signaling and inflammation, key regulator of immune cell activation.	[30]
4	PTK2	Protein Tyrosine Kinase 2 (FAK)	3.740	Controls cell adhesion, migration, and inflammatory responses via focal adhesion kinase signaling.	[31]
5	PCNA	Proliferating Cell Nuclear Antigen	3.651	Involved in DNA repair and replication, marker of cell proliferation in inflammatory tissues.	[32]
6	TOP2A	DNA Topoisomerase II Alpha	3.582	Regulates DNA replication and cell cycle; associated with hyperproliferation in RA synoviocytes.	[33]
7	RPS27A	Ribosomal Protein S27a	3.575	Involved in protein synthesis and ubiquitin conjugation, associated with immune regulation.	[34]
8	MAPK8	Mitogen-Activated Protein Kinase 8 (JNK1)	3.555	Regulates stress-induced apoptosis and inflammatory gene expression.	[35]
9	MAPK1	Mitogen-Activated Protein Kinase 1 (ERK2)	3.541	Central kinase in MAPK signaling, regulates proliferation and apoptosis in synovial cells.	[36]
10	UBC	Ubiquitin C	3.541	Participates in ubiquitin-mediated proteolysis and stress responses in inflammation.	[37]
11	CTNNB1	Catenin Beta 1 (β-catenin)	3.534	Key regulator in Wnt signaling, involved in inflammation and synovial hyperplasia.	[38]

3.4 GO and KEGG enrichment analyses of RA-related targets

To further elucidate the biological functions and signaling pathways associated with the 527 overlapping targets, GO and KEGG enrichment analyses were performed using the DAVID database. The enriched biological processes were primarily related to protein autophosphorylation, signal transduction, insulin receptor signaling and epidermal growth factor receptor pathways, indicating that the therapeutic targets were closely involved in kinase activity and receptor-mediated signaling events. In terms of cellular components, the targets were mainly localized in the extracellular exosome, cytosol, and mitochondrial matrix, suggesting their involvement in intercellular communication and energy metabolism. The molecular functions were predominantly associated with protein kinase activity, ATP binding, and protein homodimerization, further highlighting the regulation of phosphorylation-dependent signaling (Fig. 1E).

The KEGG pathway enrichment analysis revealed that the intersecting targets were significantly enriched in several inflammation- and immune-related pathways, including TNF signaling, IL-17 signaling, Toll-like receptor signaling, NOD-like receptor signaling, and Cytokine-cytokine receptor interaction, which are closely associated with the pathogenesis of RA. Additionally, pathways such as Apoptosis, p53, and Relaxin signaling were also enriched, reflecting the dual involvement of these targets in both cell survival regulation and immune modulation. Collectively, these findings indicate that the LGT-YYH herbal pair exerts anti-RA effects primarily by modulating multiple inflammatory and immune signaling pathways (Fig. 1F).

3.5 Molecular docking validation of key therapeutic targets

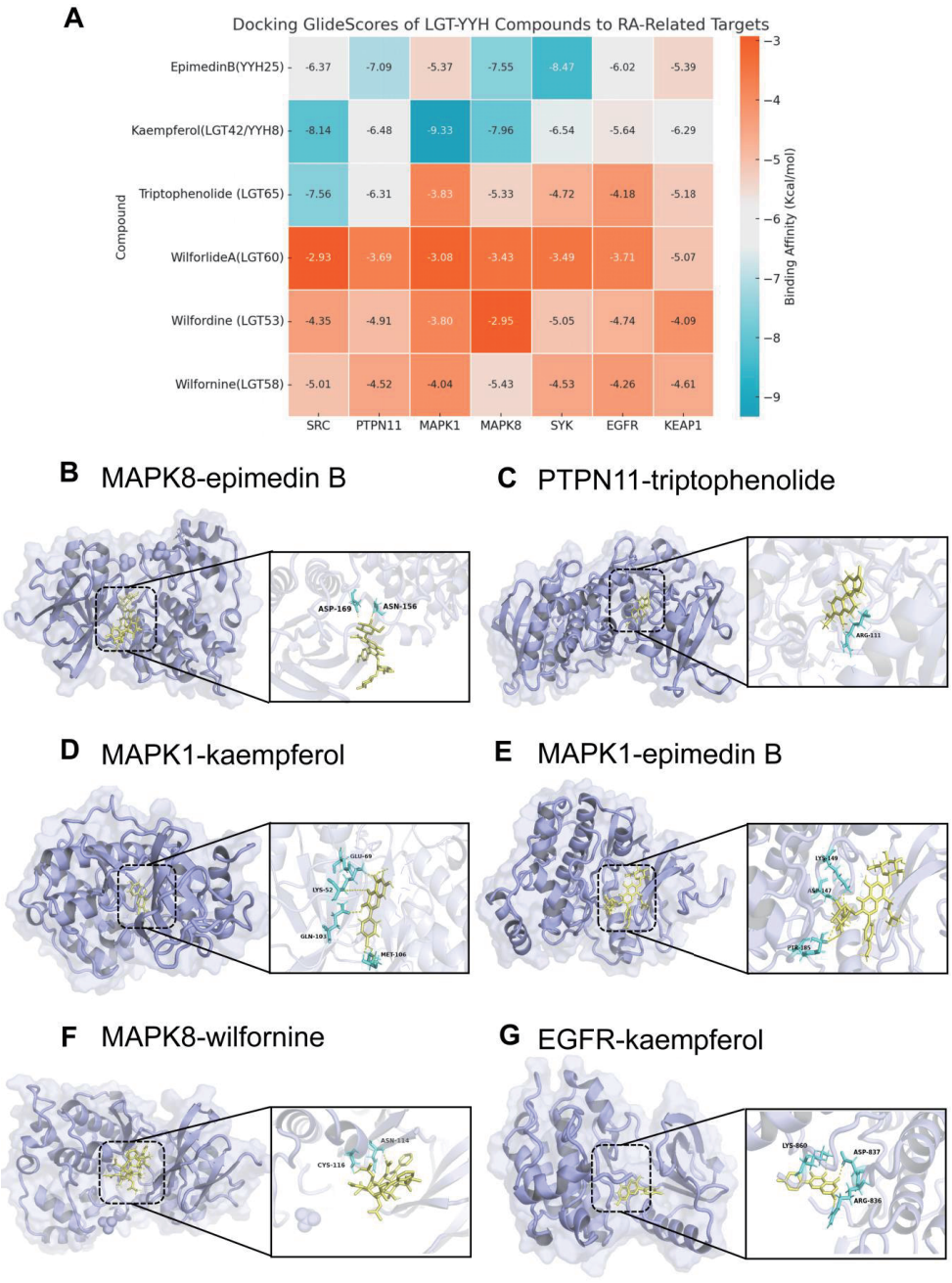
To provide structural insights into the predicted compound-target interactions, molecular docking was performed. Six high-degree compounds from the network—wilfornine (LGT58, degree 149), wilfordine (LGT53, 144), triptophenolide (LGT65, 118), wilforlide A (LGT60, 117), epimedin B (YYH25, 107), and kaempferol (LGT42/YYH8, 92)—were docked against eight key RA-related hub proteins SRC (PDB:1Y57), PTPN11/SHP2 (PDB:8U7W), MAPK1/ERK2 (PDB:8U8J), MAPK8/JNK1 (PDB:2H96), SYK (PDB:4XG9), EGFR (PDB:2J5F), KEAP1 (PDB:6ROG).

The Glide docking scores (GScore) revealed specific binding affinities between key compounds and RA-related targets. Notably, kaempferol exhibited strong binding affinities with MAPK1 (−9.33 kcal/mol), MAPK8 (−7.96 kcal/mol), and SRC (−8.14 kcal/mol), suggesting its potential to interact with multiple kinases involved in inflammatory signaling. In addition, epimedin B showed relatively strong binding with SYK (−8.47 kcal/mol), while epimedin B demonstrated favorable interactions with KEAP1 and EGFR, indicating potential involvement in redox regulation and receptor-mediated signaling (Fig. 2A).

Detailed binding mode analysis showed that these compounds formed stable interactions within the active sites of their respective targets, primarily through hydrogen bonds and hydrophobic contacts (Fig 2B-G).

Notably, the engagement of KEAP1 by wilforlide A/triptophenolide links docking to the GO/KEGG findings (oxidative stress defense), providing structural support for the proposed efficacy-detoxification synergy. Indeed, research has indicated that NRF2-KEAP1 pathway can alleviate RA.

Overall, the docking results suggest that LGT-YYH compounds may interact with key nodes in MAPK signaling and redox regulation. However, these findings primarily provide preliminary structural evidence and require further experimental validation.



(A) Heatmap of Glide docking scores (GScore) showing predicted binding affinities between selected ligands (epimedin B, kaempferol, triptophenolide, wilforlide A, wilfordine, wilfornine) and RA-related target proteins (SRC, PTPN11, MAPK1, MAPK8, SYK, EGFR, KEAP1); more negative GScore values indicate stronger predicted binding; (B) Docking model of epimedin B on MAPK8 (PDB:2H96); (C) Docking model of triptophenolide on PTPN11 (PDB:8U7W); (D) Docking model of kaempferol on MAPK1 (PDB:8U8J); (E) Docking model of epimedin B on MAPK1 (PDB:8U8J); (F) Docking model of wilfornine on MAPK8 (PDB:2H96); (G) Docking model of kaempferol on EGFR (PDB:2J5F).

Fig. 2 Molecular docking validation of key therapeutic targets in RA treatment

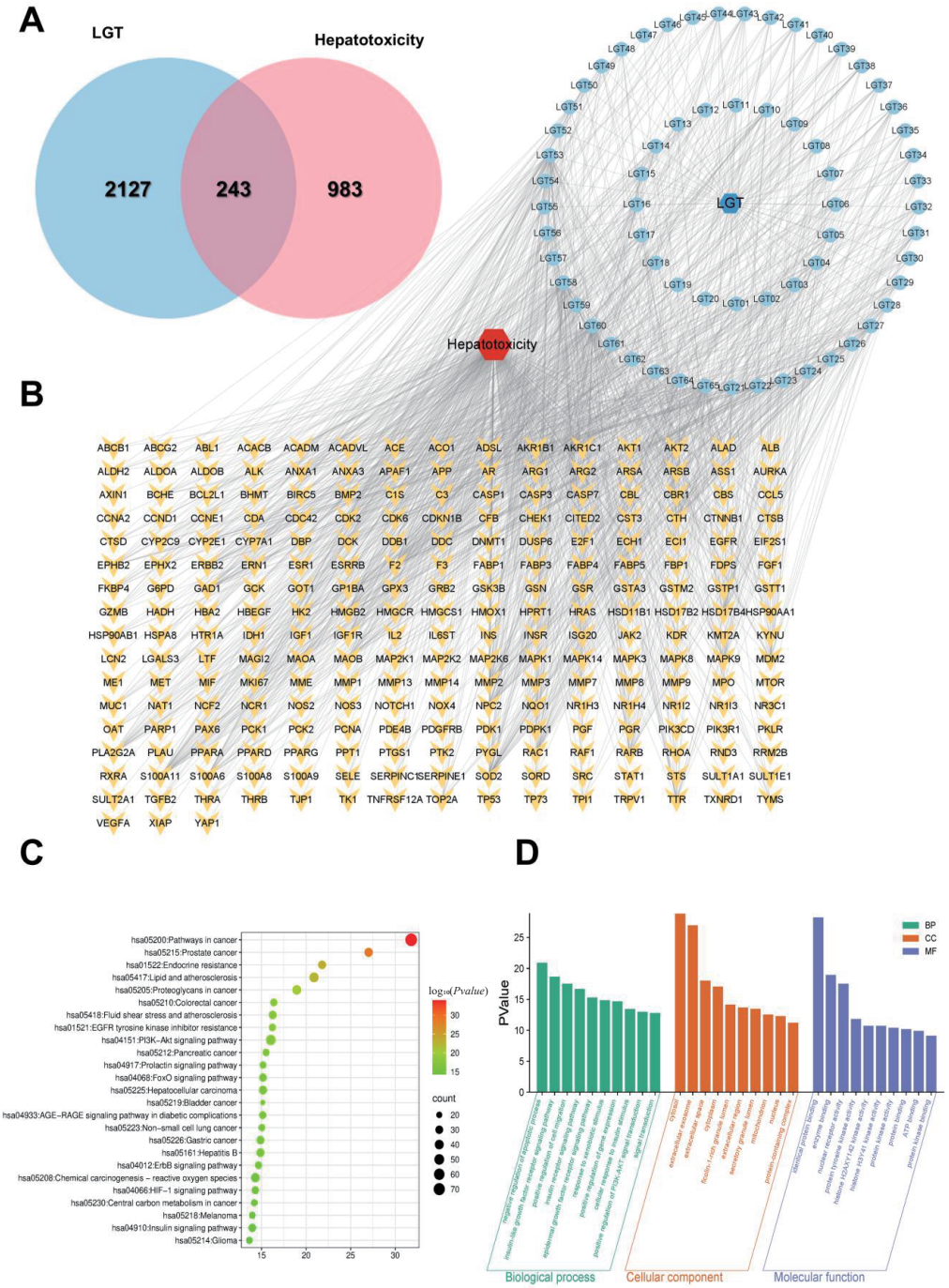
3.6 Identification of hepatotoxicity-associated targets of LGT

To identify the potential hepatotoxicity-related targets of LGT, we systematically identified its potential hepatotoxicity targets. Intersection analysis between the 2,370 LGT protein targets and a consolidated set of hepatotoxicity-related protein targets from public databases yielded 243 overlapping targets (Fig. 3A). The PPI network from these targets revealed significant protein associations crucial for understanding hepatotoxicity mechanisms (Fig. 3B). Hub protein targets analysis pinpointed TP53, INS, ALB, AKT1, CTNNB1, and ESR1 as the most central players in this hepatotoxicity network (Table 2).

Table 2 Network of the top 6 hub targets (TP53, INS, ALB, AKT1, CTNNB1, ESR1) identified using cytoHubba analysis with multiple centrality metrics (MCC, EPC, MNC, and Bottleneck)

Rank	Protein targets symbol	Consensus score
1	TP53	3.983
2	INS	3.975
3	ALB	3.975
4	AKT1	3.959
5	CTNNB1	3.938
6	ESR1	3.925

KEGG enrichment analysis of these targets highlighted pathways directly linked to liver damage, the top pathways enriched with hepatotoxicity-related targets including pathways in Cancer, PI3K-Akt signaling, TNF signaling, and Hepatocellular carcinoma, among others. These pathways are directly associated with liver cell apoptosis, inflammation, and oxidative damage. Additionally, GO enrichment analysis shows that the enriched BP including protein autophosphorylation, positive regulation of protein phosphorylation, and protein kinase activity, all of which are essential for cell signaling and metabolism. CC such as extracellular exosome and cytoplasm were significantly enriched, indicating the involvement of these cellular structures in the hepatotoxic process. Moreover, MF such as identical protein binding and protein kinase activity further underscore the role of signaling pathways in liver injury. These results demonstrate that the hepatotoxicity of LGT is likely mediated by a complex network of signaling pathways that involve cell survival, oxidative stress, and inflammatory processes, all of which are reflected in the enriched KEGG and GO terms (Fig. 3C-D).



(A) Venn diagram showing the intersection between LGT compound-related targets and hepatotoxicity-associated targets, with 243 overlapping targets identified as key targets; (B) PPI network of the 243 overlapping targets, visualized in Cytoscape, with blue nodes representing LGT compounds and yellow nodes representing shared targets; (C) KEGG enrichment bubble plot of the top 20 pathways related to hepatotoxicity, including immune response, apoptosis, and cell signaling, with bubble size indicating gene count and color intensity representing $-\log_{10}(p)$; (D) GO enrichment bar plot showing the top 10 terms in Biological Process, Cellular Component, and Molecular Function categories for hepatotoxicity-related targets.

Fig. 3 Identification of hepatotoxicity-related targets of LGT

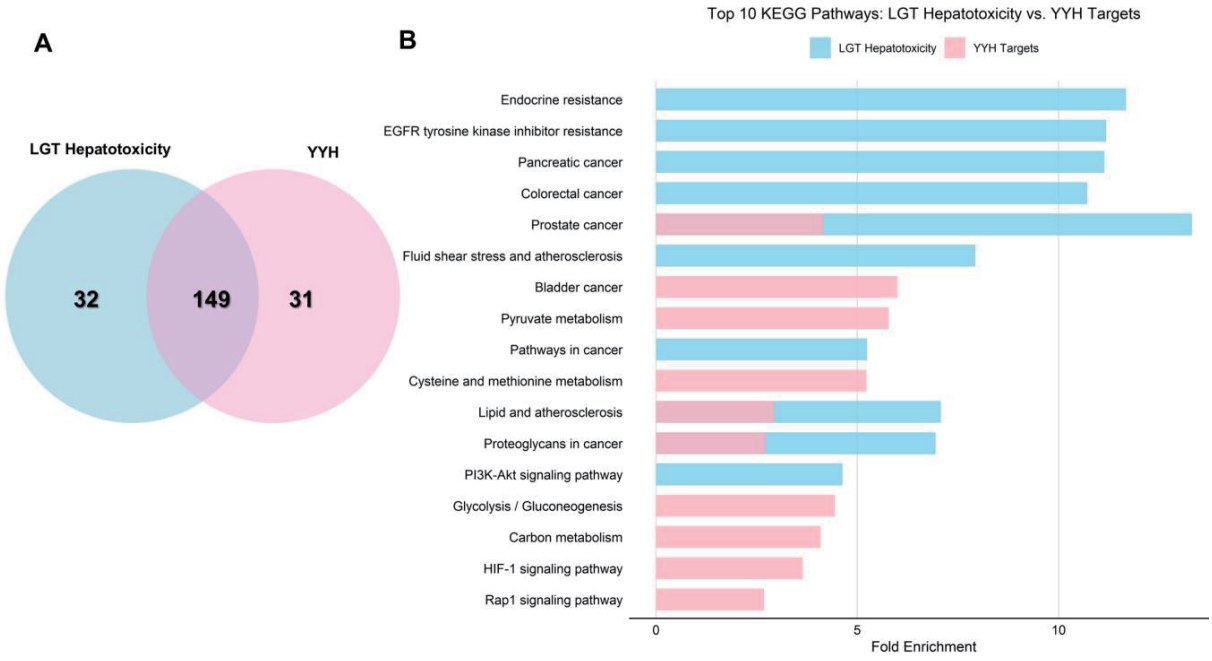
3.7 KEGG pathway enrichment analysis reveals YYH hepatoprotective potential

Previous reports have indicated that a component of YYH, icariin, exhibits hepatoprotective effects. However, it remains unclear whether it can protect against hepatotoxicity induced by LGT [39]. Furthermore, kaempferol has been demonstrated to ameliorate CCl_4-induced hepatotoxicity through modulation of AMPK/Nrf2 signaling pathways. These studies support the possibility that YYH may interact with oxidative stress-related and inflammation-related pathways involved in hepatotoxicity, which is consistent with the AKT1/ESR1/Nrf2-related signaling axis predicted in our network analysis [40]. The KEGG pathway analysis of the LGT hepatotoxicity-related targets and YYH targets revealed several overlapping and unique pathways that may suggest a compensatory role of YYH in mitigating LGT-induced hepatotoxicity. This analysis revealed 149 pathways common to both, 32 unique to LGT hepatotoxicity, and 31 unique to YYH (Fig. 4A). The targets of YYH are highly coincident with LGT hepatotoxicity-related targets, suggesting that YYH has the potential to mitigate LGT-induced hepatotoxicity.

KEGG enrichment analysis further corroborated these findings, which summarizes the top 10 significantly enriched pathways associated with LGT hepatotoxicity and YYH targets (Fig. 4B). Notably, pathways implicated in metabolic regulation, such as amino sugar and nucleotide sugar metabolism and tyrosine metabolism, as well as those involved in immune and inflammatory responses, including the VEGF and TNF signaling pathways, were significantly enriched in both networks. These overlapping enrichments suggest that both LGT and YYH may exert their effects through common metabolic and immunomodulatory mechanisms, highlighting potential nodes of interaction between toxicity and protection.

Beyond the shared pathways, the distinct pathways uniquely enriched in each network provided further mechanistic insights. LGT hepatotoxicity was specifically associated with pathways related to apoptosis and oncogenesis—including “Pathways in cancer”, “Hepatocellular carcinoma” and “Non-small cell lung cancer”—underscoring the role of LGT in promoting cell death and carcinogenic processes in the liver. In contrast, YYH-specific pathways, such as “Endocrine resistance” and “Prolactin signaling” were identified, suggesting their potential involvement in compensatory survival mechanisms and hepatoprotection (Fig. 4B).

Furthermore, the pathway comparison between the KEGG pathways of LGT hepatotoxicity and YYH targets enabled us to identify potential pathways where YYH may “negatively regulate” or “compensate” LGT toxicity. This comparison is valuable in pinpointing specific candidate pathways and proteins for molecular docking validation to further explore the mechanistic interactions between YYH and LGT in liver injury. A comprehensive comparison of all enriched KEGG pathways between LGT-associated hepatotoxicity and YYH targets is presented in Supplementary Fig. S2.



(A) Venn diagram illustrating the overlap of KEGG pathways between LGT hepatotoxicity and YYH targets. The diagram shows 149 shared pathways, 32 unique to LGT, and 31 unique to YYH; (B) Top 10 KEGG pathways for LGT hepatotoxicity and YYH targets.

Fig. 4 Comparative KEGG pathway analysis of LGT hepatotoxicity and YYH targets

3.8 Molecular docking confirms YYH compound binding to Hepatotoxicity targets

To validate the hepatoprotective potential of YYH compounds, we performed a molecular docking analysis with key hepatotoxicity-related targets. The docking was carried out using the Schrödinger software suite and Glide scoring function, with the goal of determining the binding affinities of selected YYH compounds to toxicity-related targets identified in the previous KEGG pathway comparison.

The six compounds selected for docking were chosen with multiple convergent criteria: (a) high relative abundance or marker status in YYH; (b) structural diversity covering glycosides vs. aglycones, prenylated vs. non-prenylated flavonoids, and variations in hydroxyl/methoxy substitutions; (c) literaturebacked hepatoprotective/antiinflammatory evidence; and (d) molecular properties conducive to docking studies, such as appropriate size, hydrogen-bonding capacity, and lipophilicity.

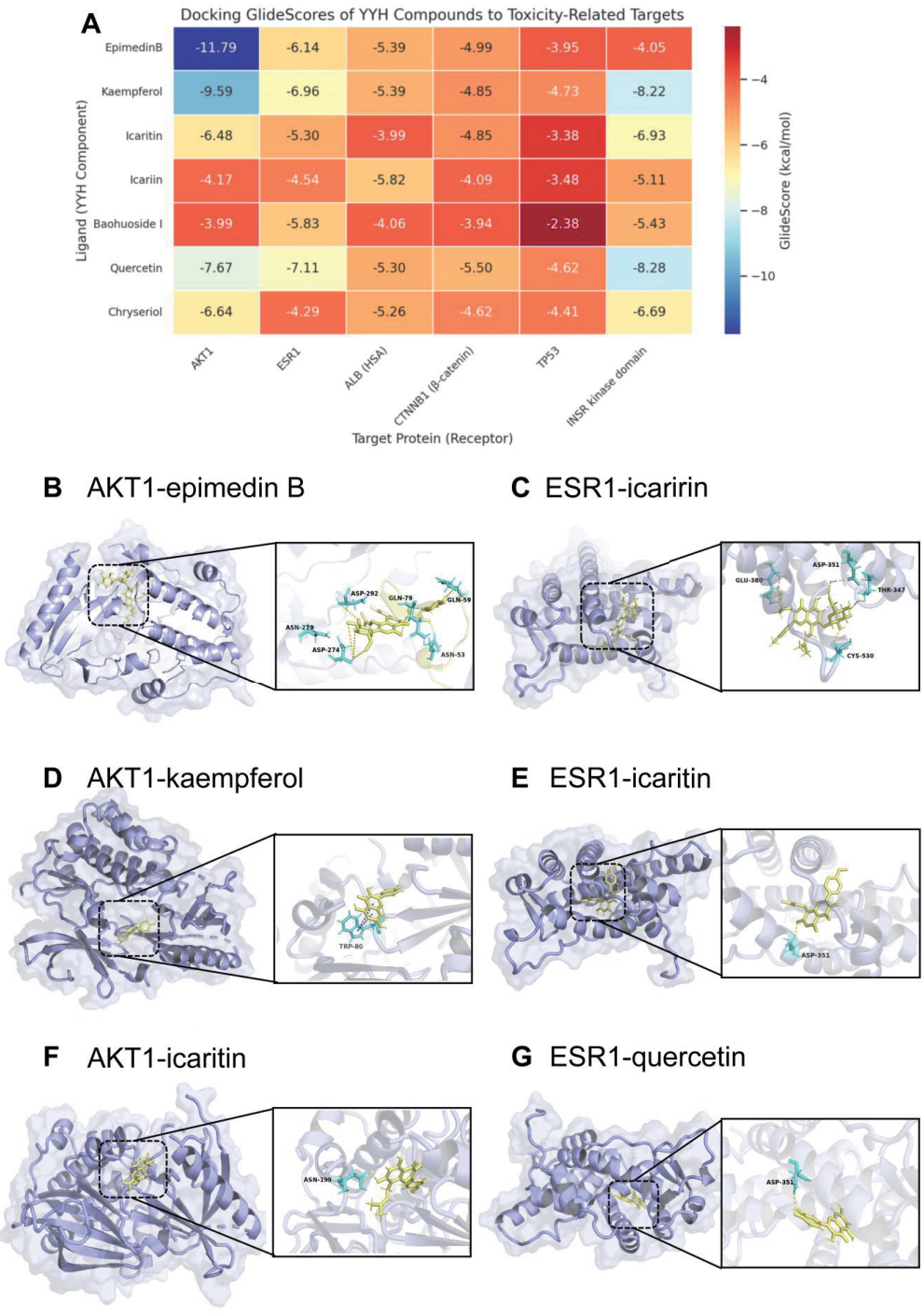
Specifically, icariin was included as a major flavonoid glycoside in YYH and a biosynthetic precursor to icaritin. Icaritin, the aglycone derivative, offers enhanced lipophilicity and has demonstrated hepatoprotective effects in acute liver injury models [12]. Baohuoside I (icariside II), another prenylated flavonoid glycoside, was selected to assess the influence of glycosylation on target binding [41]. Epimedin B, a prevalent glycosylated flavonoid in YYH, further represents the structural diversity of the herb [42]. Kaempferol, a well-studied non-prenylated flavonoid aglycone, exhibits documented activity via SIRT1/AMPK and TLR4/NF-κB pathways [8,43]. Finally, chrysoeriol, a

3′-methoxy derivative of kaempferol, was chosen to probe the effect of methoxy substitution on binding interactions [44].

The compounds selected for docking were chosen based on the following key criteria: (a) pathway consistency with hepatotoxicity-related pathways identified in KEGG enrichment and comparative analyses, which are critically involved in inflammation, oxidative stress, and cell survival during liver injury; (b) strong literature-supported evidence of hepatoprotective and anti-inflammatory activities, underscoring their potential to mitigate liver damage; (c) molecular docking feasibility, considering polarity, molecular volume, and chemical features conducive to forming hydrogen bonds or hydrophobic interactions with target proteins. Based on these criteria, the final protein targets selected for docking included AKT1 (PDB:3O96), ESR1 (PDB:3ERT), ALB (PDB:1AO6), CTNNB1 (PDB:1G3J), TP53 (PDB:2J1X), and INS (PDB:5E1S), to investigate their interactions with key hepatotoxicity-related targets.

Molecular docking revealed strong binding affinities between YYH compounds and hepatotoxicity-related targets (Fig. 5A). Icaritin, an aglycone form of icariin, exhibited even higher binding affinity with AKT1 (GScore = −6.48 Kcal/mol) and ESR1 (GScore = −5.30 Kcal/mol) As previously reported, icariin and its metabolites can protect against liver injury through multiple pathways, including the AKT signaling pathway [12]. epimedin B, a major component of YYH, demonstrated strong interactions with AKT1 (GScore = −11.79 Kcal/mol). epimedin B inhibits the activation of PI3K-AKT signaling pathways and activates the AMPK-Nrf2 signaling pathway to reduce ROS production, supporting its hepatoprotective and anti-inflammatory potential [42]. Kaempferol, a widely studied flavonoid, showed good docking results with AKT1 (GScore = −9.59 Kcal/mol) and ESR1 (GScore = −6.96 Kcal/mol). Quercetin, a flavonoid compound in YYH, showed a strong binding affinity to ESR1 (GScore = −7.11 Kcal/mol), in a study of bone-metabolism natural compounds, suggesting that ESR1 is a plausible molecular target for quercetin phytoestrogenic effects. Finally, chrysoeriol exhibited favorable binding to AKT1 (GScore = −6.64 Kcal/mol) and ESR1 (GScore = −4.29 Kcal/mol). Indeed, chrysoeriol attenuates methotrexate-induced liver injury by inhibiting PI3K-Akt pathway, reinforcing its anti-inflammatory and hepatoprotective potential [45]. Since baohuoside I did not demonstrate significant binding affinity, further investigation was not pursued.

The docking results strongly support the hypothesis that YYH compounds can alleviate liver injury by modulating key cellular pathways related to oxidative stress, inflammation, and cell survival, thus demonstrating their hepatoprotective effects and validating the potential of these compounds in reducing liver toxicity.



(A) Heatmap of Glide docking scores (GScore) showing predicted binding affinities between selected ligands (icariin, icaritin, baohuoside I, epimedin B, kaempferol, chrysoeriol, quercetin) and hepatoprotective target proteins (AKT1, ESR1, ALB, CTNNB1, TP53, INSR; (B) Docking model of epimedin B on AKT1 (PDB:3O96); (C) Docking model of icaritin on ESR1 (PDB:3ERT); (D) Docking model of kaempferol on AKT1 (PDB:3O96); (E) Docking model of icaritin on ESR1 (PDB:3ERT); (F) Docking model of icaritin on AKT1 (PDB:3O96); (G) Docking model of quercetin on ESR1 (PDB:3ERT).

Fig. 5 Docking GlideScores of YYH Compounds to Toxicity-Related Targets

4 Discussion

This study provides valuable insights into the synergistic effects and hepatotoxicity attenuation mechanisms of the LGT and YYH herbal pair in treating RA. By integrating network pharmacology and molecular docking approaches, we have identified key targets and underlying mechanisms that contribute to both the efficacy and safety of this herb pair.

The therapeutic effects of LGT-YYH are primarily mediated by a multi-target, multi-pathway approach [46]. Enrichment analysis revealed critical targets, including PTPN11, SRC, EGFR, MAPK1 and MAPK8, that are significantly involved in inflammatory and immune-related pathways, notably the MAPK signaling pathways. In addition to the MAPK pathway, other inflammation-related pathways from KEGG enrichment analysis likely contribute to the LGT-YYH herbal pair's therapeutic effects in RA. The TNF, IL-17, Toll-like receptor, and NOD-like receptor signaling pathways were significantly enriched among the intersecting targets. These pathways regulate inflammatory responses and immune dysfunction in RA [47-48].

Previous studies have demonstrated that major active components of LGT exhibit significant anti-inflammatory activities through these pathways. Triptolide and celastrol were reported to suppress NF-κB, MAPK, and pro-inflammatory cytokine signaling, including TNF-α, IL-1β, and IL-6 pathways in RA models [49]. Furthermore, wilforine was shown to alleviate RA progression through regulation of the Wnt11/β-catenin signaling pathway and inhibition of fibroblast-like synoviocyte activation [50]. Similarly, active compounds from YYH also exhibit anti-RA and anti-inflammatory activities through multiple signaling pathways. Icariin has been reported to suppress inflammatory responses in TNF-α-stimulated RA fibroblast-like synoviocytes via regulation of the TRIB1/TLR2/NF-κB signaling pathway [51]. In addition, flavonoids such as quercetin can inhibit MAPK and NF-κB activation and reduce the expression of inflammatory mediators, including IL-6 and TNF-α [52].

Therefore, the KEGG enrichment results combined with previous pharmacological evidence suggest that the therapeutic effects of LGT-YYH in RA are not limited to MAPK signaling alone but involve coordinated regulation of multiple inflammatory and immune-related pathways. This multi-pathway regulatory mode is consistent with the holistic and synergistic characteristics of traditional Chinese medicine.

A pivotal finding of this research is the identification of YYH's hepatoprotective role against LGT-induced liver injury. By analyzing the overlapping targets between LGT and hepatotoxicity-related protein targets, we predicted AKT1, ESR1, ALB, CTNNB1, and TP53 as the central mediators of the hepatotoxicity network. These targets are associated with crucial pathways, such as the PI3K-Akt and cancer pathways, which play significant roles in liver cell survival and oxidative stress. The docking results revealed that key bioactive components of YYH, including icariin, icaritin, and epimedin B, exhibit strong binding affinities for AKT1 and ESR1 [10,12,42]. This suggests that YYH may exert its protective effects primarily by modulating the AKT1-ESR1-Nrf2 antioxidant signaling axis, thereby enhancing hepatocyte survival and counteracting the oxidative stress and liver injury caused by LGT.

Previous studies have reported that icariin exhibits hepatoprotective effects through regulation of oxidative stress-related and inflammation-related pathways, particularly Nrf2-associated signaling, although whether it directly protects against LGT-induced hepatotoxicity remains unclear [12]. In addition, kaempferol has been shown to ameliorate experimental liver injury through modulation of AMPK/Nrf2 pathways [53]. These findings provide supportive biological plausibility for the

AKT1/ESR1/Nrf2-related signaling axis predicted in our network analysis. However, the proposed hepatoprotective role of YYH should be interpreted cautiously because network pharmacology identifies pathway associations without indicating regulatory directionality. Therefore, pathway overlap alone cannot demonstrate that YYH reverses LGT-induced toxic signaling, and further *in vitro* and *in vivo* studies are required to validate whether YYH-derived compounds truly attenuate LGT-induced hepatotoxicity and to clarify the regulatory direction of the identified pathways.

Our results illustrate a distinct functional differentiation between the two herbs: LGT mainly inhibits pro-inflammatory pathways to treat RA, while YYH primarily targets antioxidant and cellular survival pathways to protect the liver. This complementary mechanism, synergistic efficacy coupled with toxicity reduction, exemplifies the traditional Chinese medicine principle of "efficacy-toxicity attenuation".

5 Conclusion

The combined application of network pharmacology and molecular docking establishes a robust framework for understanding the therapeutic effects of LGT-YYH through a multi-target network centered on hub targets like PTPN11, SRC, and MAPK1/8, primarily modulating the MAPK signaling pathway. Concurrently, YYH components mitigate LGT-induced hepatotoxicity by targeting the AKT1-ESR1-Nrf2 axis, illustrating the traditional Chinese medicine principle of efficacy enhancement and toxicity reduction. A schematic summary of the proposed therapeutic and protective mechanisms of the LGT-YYH herb pair is presented in Fig. 6. These integrated network pharmacology and molecular docking results provide a mechanistic foundation for the rational clinical application of this herb pair, warranting further experimental and clinical validation.

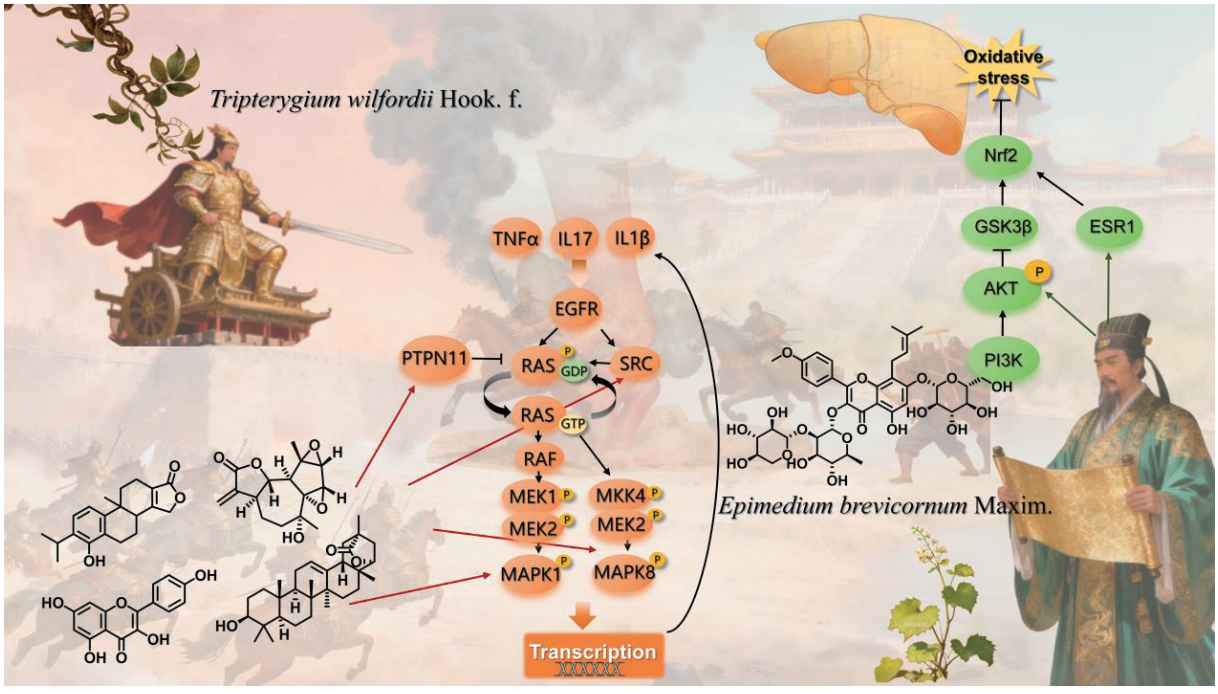


Fig. 6 Graphical summary of the multi-target, multi-pathway mechanisms of LGT-YYH in RA and hepatoprotection

References

[1] Liu X, Wang Z, Qian H, et al. Natural medicines of targeted rheumatoid arthritis and its action mechanism. Front Immunol, 2022, 13: 945129.

[2] Shan Y, Zhao J, Wei K, et al. A comprehensive review of tripterygium wilfordii hook. f. in the treatment of rheumatic and autoimmune diseases: bioactive compounds, mechanisms of action, and future directions. Front Pharmacol, 2023, 14: 1282610.

[3] Kciuk M, Garg A, Rohilla M, et al. Therapeutic potential of plant-derived compounds and plant extracts in rheumatoid arthritis-comprehensive review. Antioxid (basel Switz), 2024, 13: 775.

[4] Zhou YY, Xia X, Peng WK, et al. The effectiveness and safety of tripterygium wilfordii hook. F extracts in rheumatoid arthritis: a systematic review and meta-analysis. Front Pharmacol, 2018, 9: 356.

[5] Wang J, Chen N, Fang L, et al. A systematic review about the efficacy and safety of tripterygium wilfordii hook.f. Preparations used for the management of rheumatoid arthritis. Evid-based Complement Altern Med: Ecam, 2018, 2018: 1567463.

[6] Chen K, Chen X, Huang S, et al. Therapeutic effects and mechanisms of tripterygium wilfordii extracts in rheumatoid arthritis: a systematic review and meta-analysis of preclinical studies. Sci Rep, 2025, 15: 27960.

[7] Zhou GL, Su SL, Yu L, et al. Exploring the liver toxicity mechanism of tripterygium wilfordii extract based on metabolomics, network pharmacological analysis and experimental validation. J Ethnopharmacol, 2025, 337: 118888.

[8] Li M, Luo Q, Chen X, et al. Screening of major hepatotoxic components of Tripterygium wilfordii based on hepatotoxic injury patterns. BMC Complementary Med Ther, 2023, 23: 9.

[9] Ma H, He X, Yang Y, et al. The genus Epimedium: an ethnopharmacological and phytochemical review. J Ethnopharmacol, 2011, 134: 519-41.

[10] Zhang J, Fan F, Liu A, et al. Icariin: a potential molecule for treatment of knee osteoarthritis. Front Pharmacol, 2022, 13: 811808.

[11] He X, Wu T, He H, et al. Study of kaempferol in the treatment of rheumatoid arthritis through modulation of the NLRP3/CASP1/GSDMD axis and T-cell activation: based on network pharmacology, single-cell analysis, and experimental validation. Int Immunopharmacol, 2024, 143: 113357.

[12] Ma Y, Sun F, Zhang E, et al. Efficacy and mechanism of nourishing yin and purging fire therapy for central precocious puberty based on meta-analysis and network pharmacology. Medicine, 2023, 102: e36395.

[13] Jie H, Wu Q. Treating 47 cases of RA by Jinguan tablet. Clin J Chin Med, 2012, 4: 58.

[14] Ding C, Liu Q, You X, et al. Investigating the molecular mechanism of epimedium herb in treating rheumatoid arthritis through network pharmacology, molecular docking, and experimental validation. Mol Diversity, 2025, 29: 4061-81.

[15] Ru J, Li P, Wang J, et al. TCMSP: a database of systems pharmacology for drug discovery from herbal medicines. J Cheminf, 2014, 6: 13.

[16] Wang X, Shen Y, Wang S, et al. PharmMapper 2017 update: a web server for potential drug target identification with a comprehensive target pharmacophore database. Nucleic Acids Res, 2017, 45: W356-W360.

[17] Ahmad S, Jose da Costa Gonzales L, Bowler-Barnett EH, et al. The UniProt website API: facilitating programmatic access to protein knowledge. Nucleic Acids Res, 2025, 53: W547-W553.

[18] Delgado-Arévalo C, Calvet-Mirabent M, Triguero-Martínez A, et al. NLRC4-mediated activation of CD1c+ DC contributes to perpetuation of synovitis in rheumatoid arthritis. JCI Insight, 2022, 7: e152886.

[19] Amberger JS, Hamosh A. Searching online mendelian inheritance in man (OMIM): a knowledgebase of human genes and genetic phenotypes. Curr Protoc Bioinform, 2017, 58: 1.2.1-1.2.12.

[20] Stelzer G, Rosen N, Plaschkes I, et al. The GeneCards suite: from gene data mining to disease genome sequence analyses. Curr Protoc Bioinform, 2016, 54:

1.30.1-1.30.33.

[21] Wiegers TC, Davis AP, Wiegers J, et al. Integrating AI-powered text mining from PubTator into the manual curation workflow at the Comparative Toxicogenomics Database. Database: J Biol Databases Curation, 2025, 2025: baaf013.

[22] Zhou Y, Zhang Y, Zhao D, et al. TTD: therapeutic target database describing target druggability information. Nucleic Acids Res, 2024, 52: D1465-D1477.

[23] Bardou P, Mariette J, Escudié F, et al. jvenn: an interactive venn diagram viewer. BMC Bioinf, 2014, 15: 293.

[24] Song L, Qian W, Yin H, et al. TCMSTD 1.0: a systematic analysis of the traditional chinese medicine system toxicology database. Science China Life Sci, 2023, 66: 2189-92.

[25] Ono K, Fong D, Gao C, et al. Cytoscape web: bringing network biology to the browser. Nucleic Acids Res, 2025, 53: W203-W212.

[26] Szklarczyk D, Kirsch R, Koutrouli M, et al. The STRING database in 2023: protein-protein association networks and functional enrichment analyses for any sequenced genome of interest. Nucleic Acids Res, 2023, 51: D638-D646.

[27] Dennis G Jr, Sherman BT, Hosack DA, et al. DAVID: database for annotation, visualization, and integrated discovery. Genome Biol, 2003, 4: 3.

[28] Tartaglia M, Martinelli S, Stella L, et al. Diversity and functional consequences of germline and somatic PTPN11 mutations in human disease. Am J Hum Genet, 2006, 78: 279-90.

[29] Roskoski R. Src protein-tyrosine kinase structure, mechanism, and small molecule inhibitors. Pharmacol Res, 2015, 94: 9-25.

[30] Clark DN, Begg LR, Filiano AJ. Unique aspects of IFN-γ/STAT1 signaling in neurons. Immunol Rev, 2022, 311: 187-204.

[31] Feng A, Caro YM, Gardner C, et al. PTK2-associated gene signature could predict the prognosis of IPF. Respir Res, 2023, 24: 304.

[32] González-Magaña A, Blanco FJ. Human PCNA structure, function and interactions. Biomolecules, 2020, 10: 570.

[33] Liu G, Lin W, Zhang K, et al. Elucidating the prognostic and therapeutic significance of TOP2A in various malignancies. Cancer Genet, 2024, 288-289: 68-81.

[34] Luo JS, Zhao H, Chen LX, et al. Multifaceted functions of RPS27a: an unconventional ribosomal protein. J Cell Physiol, 2023, 238: 485-97.

[35] Xu P, Zhang G, Hou S, et al. MAPK8 mediates resistance to temozolomide and apoptosis of glioblastoma cells through MAPK signaling pathway. Biomed Pharmacother = Biomed Pharmacother, 2018, 106: 1419-27.

[36] Wang Y, Guo Z, Tian Y, et al. MAPK1 promotes the metastasis and invasion of gastric cancer as a bidirectional transcription factor. BMC Cancer, 2023, 23: 959.

[37] Bianchi M, Crinelli R, Arbore V, et al. Induction of ubiquitin C (UBC) gene transcription is mediated by HSF1: role of proteotoxic and oxidative stress. FEBS Open Bio, 2018, 8: 1471-85.

[38] Lietman C, Wu B, Lechner S, et al. Inhibition of wnt/β-catenin signaling ameliorates osteoarthritis in a murine model of experimental osteoarthritis. JCI Insight, 2018, 3: e96308.

[39] Ma Y, Zhao C, Hu H, et al. Liver protecting effects and molecular mechanisms of icariin and its metabolites. Phytochemistry, 2023, 215: 113841.

[40] Lim DW, Lee JE, Lee C, et al. Natural products and their neuroprotective effects in degenerative brain diseases: a comprehensive review. Int J Mol Sci, 2024, 25: 11223.

[41] Ni HTN, Linh NN, Nhung PTT, et al. Icariside II: natural occurrence, biotransformation, pharmacological activity, synthetic modification, pharmacokinetics, and bioavailability. J Pharm Pharmacol, 2025, 77: 1491-1512.

[42] Lai Y, Li H, Zhou T, et al. Epimedin B attenuates ovariectomy-induced bone loss by suppressing osteoclastogenesis through decreasing ROS production and targeting ESR1. Free Radical Biol Med, 2025, 240: 347-63.

[43] Du YC, Lai L, Zhang H, et al. Kaempferol from penthorum chinense pursh suppresses HMGB1/TLR4/NF-κB signaling and NLRP3 inflammasome activation in acetaminophen-induced hepatotoxicity. Food Funct, 2020, 11: 7925-34.

[44] Aboulaghras S, Sahib N, Bakrim S, et al. Health benefits and pharmacological aspects of chrysoeriol. Pharm (Basel Switz.), 2022, 15: 973.

[45] Li L, Ju J, Zhuang X, et al. Chemistry of bairui granules and its mechanisms in the protective effect against methotrexate-induced liver injury. Phytomedicine: Phytomed: Int J Phytother Phytopharm, 2024, 122: 155158.

[46] Yan Q, Yao G. A network pharmacology-based study on the anti-hepatoma effect of Phellodendri Chinensis Cortex. Asian J Tradit Med, 2021, 16: 276-93.

[47] Firestein GS, McInnes IB. Immunopathogenesis of rheumatoid arthritis. Immunity, 2017, 46: 183-96.

[48] Weyand CM, Goronzy JJ. The immunology of rheumatoid arthritis. Nat Immunol, 2020, 22: 10-18.

[49] Song X, Zhang Y, Dai E. Therapeutic targets of thunder god vine (Tripterygium wilfordii hook) in rheumatoid arthritis (Review). Mol Med Rep, 2020, 21: 2303-10.

[50] Huang Y, Peng Y, Li H, et al. Wilforine inhibits rheumatoid arthritis pathology through the Wnt11/β-catenin signaling pathway axis. Arthritis Res Ther, 2023, 25: 243.

[51] Wu ZM, Xiang YR, Zhu XB, et al. Icariin represses the inflammatory responses and survival of rheumatoid arthritis fibroblast-like synoviocytes by regulating the TRIB1/TLR2/NF-kB pathway. Int Immunopharmacol, 2022, 110: 108991.

[52] Tang M, Zeng Y, Peng W, et al. Pharmacological Aspects of Natural Quercetin in Rheumatoid Arthritis. Drug Des Devel Ther, 2022, 16: 2043-53.

[53] Lee C, Yoon S, Moon JO. Kaempferol Suppresses Carbon Tetrachloride-Induced Liver Damage in Rats via the MAPKs/NF-κB and AMPK/Nrf2 Signaling Pathways. Int J Mol Sci, 2023, 24: 6900.